Variations in Nonlinearly Evolved Nearshore Spectra and Their Significance in the Estimation of Wave Forces

Serdar Beji[1] and Kazuo Nadaoka[2]

Abstract

Variability of spectral estimates is examined with respect to the nonlinearity of the wave field considered. Both measured field data and numerical simulations are used for checking the extent of variations, which are quantified as histograms that closely follow the chi-square distribution. An absolute assessment of the variations over the entire frequency band of a spectrum is also made and found to approach to a mean of 70% regardless of the frequency concerned. Finally, it is observed that a nonlinearly evolving wave field of initially constant spectral shape gradually assumes a spectral variability, which is characterized by the chi-square distribution. The last finding provides a clue for a possible cause of the variations observed in the estimates of spectra.

Introduction

Despite the important implications concerning uncertainties in the estimation of wave loads, deviations of individual spectral samples from the final spectral estimate, as computed through ensemble averaging and frequency smoothing, appear to have received little attention. Borgman (1972) questioned the validity of the use of the chi-square confidence interval for high sea conditions and tested the accuracy of the method using wave data from a hurricane. His comparison with the theory yielded some discrepancies but the overall conclusion was that the chi-square approximation was acceptable even for hurricane waves. Donelan and Pierson (1983) presented an extensive examination of wind-generated laboratory and field wave data with special emphasis on the sampling variability of the spectral peak. They showed that while the scaling according to the spectral peak would bias the spectral estimates, the sampling variability of the spectra was in good accord with the chi-square distribution. The latter finding is in line with Borgman's (1972) conclusion.

[1] Assoc. Prof., Department of Naval Architecture and Ocean Engineering, Istanbul Technical University, Maslak 80626, Istanbul, Turkey.
[2] Professor, Graduate School of Information Science and Engineering, Tokyo Institute of Technology, 2-12-1 O-okayama, Meguro-ku, Tokyo 152-8552, Japan.

It is well known that nonlinear evolutions of surface gravity waves are highly dependent on the phase values of the interacting wave components. Thus, unlike linear waves, depending solely on the initial phase values, a nonlinear random wave field of a certain spectral shape may evolve quite differently from a wave field of the same spectral shape but different initial phases. Variations in such nonlinearly evolved spectra are not negligible and therefore a closer examination may lead to interesting results. In particular, some hints as to the source of the variability observed in spectral estimates may be gained.

This work first examines the sampling variability of the spectra of field measurements in the nearshore zone (Nakamura and Katoh, 1992) and confirms that the chi-square distribution is a good approximation to these variations. The agreement with the theory is remarkable because for these highly nonlinear waves the surface displacements do not exactly satisfy the Gaussian distribution. Absolute deviations of the individual spectra from the ensembled mean are also computed for the entire frequency band and found to resemble a white-noise with a mean level of approximately 70%. The effect of nonlinearity on the spectral variability is investigated by performing a numerical test, which simulates the nonlinear evolution of an initially constant spectral shape over a gently decreasing depth. The numerical results show that the initially constant spectral shape gradually assumes a variability, which is in accord with the chi-square distribution. This finding indicates that nonlinearity may be a responsible mechanism for the observed spectral variability.

For practical applications, the crucial aspect of the spectral variability lies in the uncertainties it implies in the estimation of wave loads, which is essential for a safe design. Possible further investigations on the subject are mentioned in closing.

Analysis of Field Measurements

The spectral variations are first examined by using field data. Two particular data sets from the field measurements of Nakamura and Katoh (1992) were selected; namely, the data of 25 February 1989 and 28 February 1989. The measurements were performed at the Hazaki Oceanographical Research Facility (HORF) near Kashima, Japan. The site of the field observations was a natural sandy beach facing the Pacific Ocean. Ten ultrasonic wave gauges were used; of which seven were installed on the 427 m-long observatory pier while the remaining three were deployed at water depths of 9 m (Station 8), 14 m (Station 9), and 24 m (Station 10), located respectively at the distances 1.3, 2.1, and 3.2 km from the shoreline.

The data of 25 February 1989 was recorded prior to a storm and displayed a typical sea state with significant wave height H_s=1.5 m and period T_s=4.8 s at the offshore station (Station 10) where the waves were essentially linear. On the other hand, the data of 28 February 1989 was recorded in the aftermath of the storm and the spectrum at Station 10 represented a swell with H_s=2.2 m and T_s=12.4 s; the waves were nonlinear. While the water depths at Stations 10 to 8 were too deep to cause depth-induced breaking, most of the waves at the remaining stations were either breaking or broken.

For computations the data at each station was first segmented into $M = 12$ groups of $N = 1024$ data points and Fourier transformed. Out of the 512 unique Fourier pairs the first 256 components, which covered the frequency range of 0.0-0.5 Hz, were considered sufficient to capture almost all the wave energy present and therefore the subsequent computations were performed by using the first 256 transformed pairs.

For each separate set, comprising the Fourier components a_{nm} and b_{nm} for $n = 1,...,256$ and $m = 1,...,12$ the Fourier amplitudes $C_{nm}^2 = a_{nm}^2 + b_{nm}^2$ were frequency smoothed by a five-point running average

$$\overline{C}_{nm}^2 = \frac{1}{5} \sum_{i=n-2}^{n+2} C_{im}^2 .$$ (1)

Using the above frequency smoothed values; a segment averaging was performed

$$\hat{C}_n^2 = \frac{1}{12} \sum_{m=1}^{12} \overline{C}_{nm}^2 ,$$ (2)

which in turn could be used to obtain the spectral estimates $\hat{S}_n = \hat{C}_n^2 / \Delta f$ with $2 \times 5 \times 12 = 120$ degrees of freedom. Here, $\Delta f = 1/N\Delta t = 1.953 \times 10^{-3}$ Hz, and $\Delta t = 0.5$ s is the sampling interval.

Since it has implicity been assumed that the process is approximately Gaussian, the 90% confidence level for the estimated spectral variance with 120 degrees of freedom may be computed as (see Bendat and Piersol, 1971, p.114)

$$P\left(\frac{120\hat{S}_n}{\chi_{120;0.05}^2} < S_n < \frac{120\hat{S}_n}{\chi_{120;0.95}^2} \right) = 0.90 ,$$ (3)

where S_n is the true but unknown spectral variance corresponding to the frequency $n\Delta f$. Substituting $\chi_{120;0.05}^2 = 146.57$ and $\chi_{120;0.95}^2 = 95.70$ gives

$$P(0.82\hat{S}_n < S_n < 1.25\hat{S}_n) = 0.90 ,$$ (4)

which indicates that the true spectrum is known to within ± 25% or a range of 43% at the 90% confidence level. Figure 1 shows the estimated spectrum with 120 DOF and a single realization with 2 DOF for the data of 28 February 1989 at Station 10.
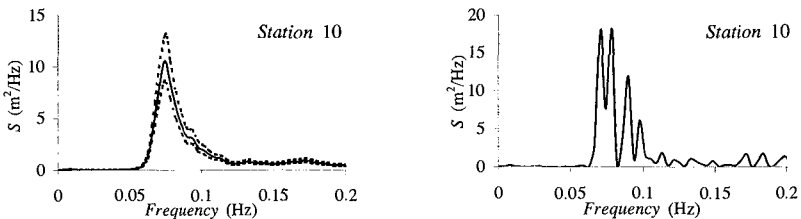
Figure 1. The spectral estimate on the left has 120 degrees of freedom and is within −18 to +25% of the true spectrum at the 90% confidence level. The 90% confidence limits are shown by dashed lines. The spectral estimate on the right is a single realization with 2 degrees of freedom.

Hypothetically, the random variable $r = C_n^2 / S_n \Delta f$ is distributed according to $\exp(-r)$ for r greater than zero. Since S_n is not known, the estimate $\hat{S}_n$ can be used for testing the hypothesis that the computed r values will follow the exponential law.

The computations were done for the data of both 25 and 28 February 1989 using all 12 segments with 256 components covering the frequency range 0.0-0.5 Hz. Consequently, 3072 values of r were obtained. Strictly speaking, vanishingly small values of $\hat{S}_n$ should have been avoided to prevent possible errors, however no problems were encountered and therefore the entire range of $\hat{S}_n$ values was used.

In Figure 2 the histograms for the 3072 values of r for a class interval 0.05 wide is shown over the range $0 < r < 5$ for three selected stations. Each histogram has been normalized by its value in the first interval (0.00-0.05).
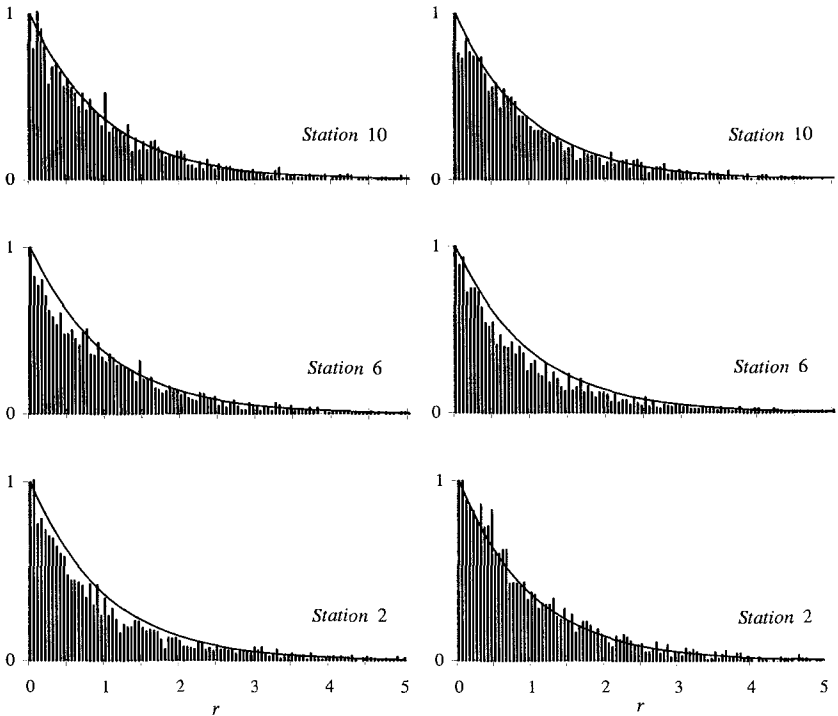
Figure 2. Normalized histograms of the ratio, r, of raw spectral estimates to the smoothed average spectral estimates for Stations 10, 6, and 2. Left column: 25 February 1989, right column: 28 February 1989. The solid line is the theoretical curve $\exp(-r)$.

In order to obtain quantitative estimates of the spectral variations, the field data is analyzed in a different manner. Instead of treating the spectral variations regardless of frequency, the mean absolute percentage of deviations from the estimate for each frequency component are computed according to the formula

$$\varepsilon_n = \frac{1}{12} \sum_{m=1}^{12} \frac{\left| \hat{S}_n - C_{nm}^2 / \Delta f \right|}{\hat{S}_n}, \tag{5}$$

and then plotted over frequency. Figure 3 shows the results corresponding to the stations shown in Figure 2.
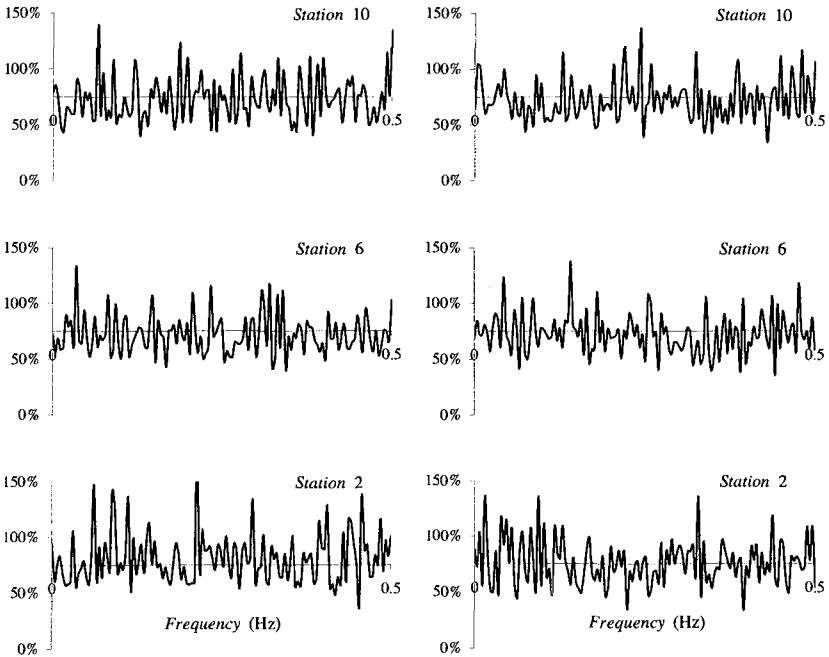
Figure 3. Mean absolute percentage of spectral variations over frequency as computed from equation (5) for the stations of Figure 2.

As it is seen from the above graphs, the mean absolute percentages of individual deviations from the estimated spectral values exhibit a random distribution over frequency with a mean of approximately 75%. Further computations have shown that the number of frequency averaging determines the exact value of the mean percentage with the trend that the higher the number of frequency merging the higher the resulting mean percentage. This is to be expected because the frequency averaging essentially pulls down the estimated spectral shape, resulting in smaller and smaller spectral values. Therefore, if a meaningful mean deviation percentage were to be obtained, it would be best not to introduce any frequency smoothing at all.

As an alternative, instead of C_{nm}^2, one could use $\overline{C}_{nm}^2$ in equation (5) to eliminate the quantitative effect of frequency smoothing. Computations without any frequency smoothing but with different number of FFT points and of ensemble averaging have yielded that the mean absolute deviations center around 70% with no sensitivity to the number of FFT points and to the number of ensemble averaging. Likewise, use of $\overline{C}_{nm}^2$ in equation (5) has yielded nearly the same numerical value for different frequency averaging operations. Thus, it has been concluded that the mean absolute deviations center around 70% with a random-noise type appearance over frequency regardless of the characteristics of the wave field considered.

A possible cause for the noise-like distribution of spectral variations over entire frequency band may be attributed to a nonlinear mechanism allowing continuous energy flow among spectral components. For testing the validity of such a notion, a numerical experiment was carried out with supportive results. The computations and results are described in detail in the following section.

A Numerical Experiment

Using a nonlinear wave model, nonlinear evolution of an initially constant spectral shape over decreasing water depth is now investigated. The wave model may be considered as a generalized KdV equation (Korteweg and de Vries, 1895), which is valid for arbitrary ratios of depth to wavelength (Nadaoka *et.al.*, 1994; Beji and Nadaoka, 1997a)

$$C_g \eta_t + \tfrac{1}{2} C_p (C_p + C_g) \eta_x - \frac{(C_p - C_g)}{k^2} \eta_{xxt} - \frac{C_p (C_p - C_g)}{2k^2} \eta_{xxx}$$
$$+ \tfrac{1}{2} [C_p(C_g)_x + (C_p - C_g)(C_p)_x] \eta + \tfrac{3}{4} g \left(3 - 2\frac{C_g}{C_p} - \frac{k^2 C_p^4}{g^2} \right) (\eta^2)_x = 0, \tag{6}$$

where C_p, C_g, and k are respectively the phase and group velocities and the wave-number computed according to the linear theory dispersion relation for a dominant wave frequency ω and a given local depth h, the subscripts x and t indicate partial differentiation with respect to space and time, respectively.

Based on the above unidirectional wave equation a spectral model was developed (Beji and Nadaoka, 1997b; 1998) resulting in a set of evolution equations describing the spatial changes of the component wave amplitudes of a prescribed incident wave field. No detail is given here; the complete derivation can be found in Beji and Nadaoka (1998). It must be indicated that the wave model itself is not crucial so long as it contains a nonlinear mechanism to generate harmonics thus allowing continuous redistribution of energy.

For numerical investigations a uniformly decreasing depth of 1:50 slope followed by a horizontal section is selected. Waves first steepen due to decreasing depth and then the energy exchange takes places as they travel over the shallow constant depth region. The water depth at the incident boundary is 25 m, which reduces to 5 m after a distance of 1000 m. For the next 1000 m, the water depth remains constant at 5 m.

The wave field at the incident boundary is assumed linear with a Bretshneider type spectral shape and a typical mean period $T_m \approx 12$ s. For ensuring the linearity of the incident wave field as well as preventing any possible breaking in the shallow region, the incident mean wave height is taken $H_m = 1.0$ m, a moderate value. Twelve realizations with *constant spectral shape* but *different initial phase* assignments are performed. As in the field measurements, the computations were done using 256 Fourier pairs with $\Delta f = 1.953 \times 10^{-3}$ Hz, and a five-point running average was applied for frequency smoothing. Thus, all the statistical values given in the previous section apply to the numerical simulations as well.

In Figure 4, the left column shows the histograms for three selected stations while the right column gives the mean absolute percentage of spectral variations for the same stations.
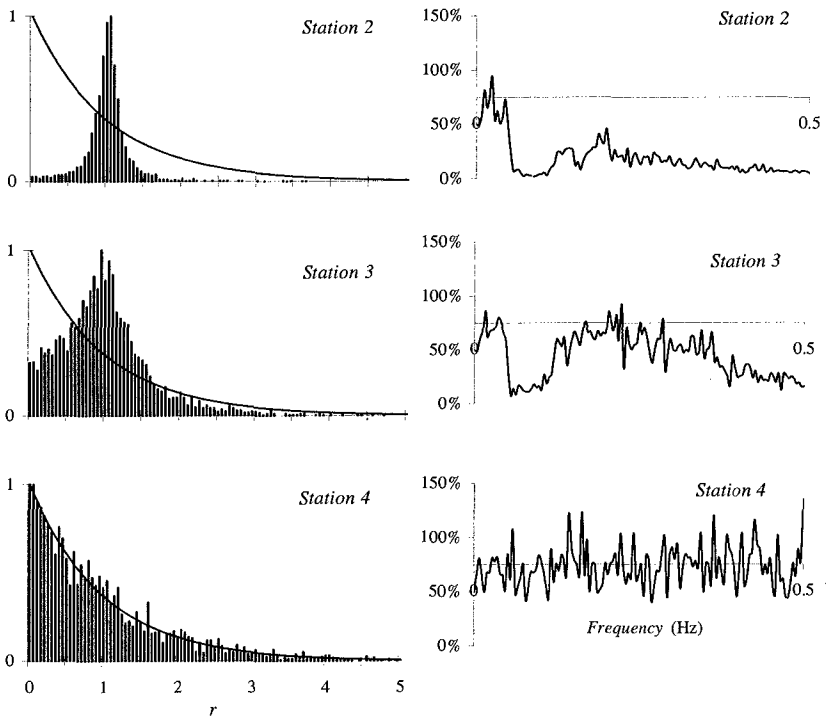
Figure 4. Histograms of spectral variability (left) and mean absolute percentage of variations (right) for an initially constant spectral form at three different locations. Station 1 (not shown) is the incident boundary at $x=0$ m and $h=25$ m; Station 2, $x=250$ m and $h=20$ m; Station 3, $x=750$ m and $h=10$ m; Station 4, $x=2000$ m and $h=5$ m. Histograms for Station 2 and 3 are normalized by their largest values whereas histogram for Station 4 is normalized by its value in the first interval, as in Figure 2.

From the graphs for Station 2 it is seen that the histogram is quite unlike the theoretical chi-square distribution (due to the initially imposed unvarying spectral heights for all realizations) but increasing nonlinearity begins manifesting itself in the lower frequency portion of the wave spectrum by introducing an appreciable variability in that particular region. At Station 3, the histogram is broader but still not quite like its theoretical shape. The effect of nonlinearity has now spread to the higher frequency part of the spectrum; however, the main frequency band (0.05-0.12 Hz), which contains the primary energy of the spectrum remains almost unaffected as can be observed by remarkably low percentages of mean absolute variations. The main frequency band is the last to be modified because the sub- and super-harmonics must reach to appreciable levels before they could interact with it. After travelling the shallow constant depth region of 1000 m, the wave field at Station 4 is completely modified by the wide-spread nonlinear interactions and it has attained a spectral variability which is in excellent agreement with the chi-square distribution. Also, the mean absolute percentages of deviations show a white-noise type random distribution over frequency with a mean of 75%, as for the field measurements given in Figure 3. The results of overall computations imply the existence of a nonlinear mechanism behind the observed spectral variability. This nonlinear mechanism needs not be in the form of a second-order nonlinearity as in here, it may be a cubic nonlinearity, *e.g.* the nonlinear Schrödinger equation, or a higher order nonlinearity that would permit energy exchange among spectral components.

While the chi-square distribution is linked to the properties of stationary Gaussian processes, the examination of the field data used here shows that this may not be strictly the case. For instance, computing the histograms for the surface elevation distributions at Stations 10 and 6 of 28 February 1989 data results in the graphs shown in Figure 5. While the distribution of Station 10 may be accepted as Gaussion, the distribution of Station 6 clearly diverges from the theoretical curve. However, the histograms of spectral variabilities for both Station 10 and Station 6 satisfy the theoretical chi-square distribution very closely, as is seen in Figure 2. This particular point was Borgman's (1972) principal motivation for investigating the validity of the chi-square confidence intervals for high sea conditions.
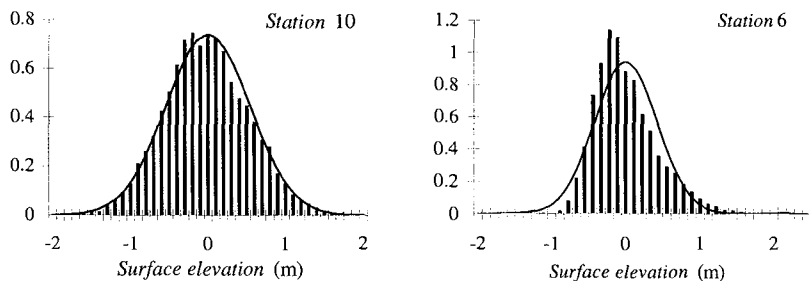
Figure 5. Histograms for distributions of surface displacements for the data of 28 February 1989 at Station 10 and Station 6.

The point that the wave field needs not be truly Gaussian in order that the corresponding spectral variations be chi-square distributed is especially mentioned here because except for a few stations of the data of 25 February 1989, almost all the other data (measured or computed) were actually representing nonlinear waves.

Concluding Remarks

Analysis of the field data comprising linear and highly nonlinear wave fields has confirmed the validity of the standard assumption that the spectral variabilities follow the chi-square distribution. It is also observed that the wave field does not necessarily need to be truly Gaussian for its spectral variability to follow the chi-square distribution. The numerical simulation of a nonlinearly evolving spectrum has shown that an initially constant spectral shape gradually assumes a variability, which is in perfect agreement with the chi-square distribution. Therefore, nonlinear interactions may be at least partially responsible for the variability observed in spectral computations. Once the spectral variability is attained, it remains preserved even if the wave field becomes linear as, for instance, by breaking or moving into deeper regions.

The quantitative assessments of the variability show that on the average 70% deviation of a spectral component from the smoothed and segment averaged value is possible. In estimating the extreme wave loads this percentage may be interpreted as an indicator of the additional transient loads. For making reliable assessments, it is necessary to investigate the actual wave load variations by performing computations with wave fields having such variable spectra.

Acknowledgments

References

Beji, S. and K. Nadaoka, 1997a. A time-dependent nonlinear mild-slope equation for water waves. *Proc. Roy. Soc. Lond. A*, **453**, 319-332.

Beji, S. and Nadaoka, K., 1997b. Spectral modelling of nonlinear shoaling and breaking over arbitrary depths. *Proc. Coastal Dynamics '97*, 285-294.

Beji, S. and K. Nadaoka, 1998. A spectral model for unidirectional nonlinear wave propagation over arbitrary depths. *Coastal Engng.*, Submitted.

Bendat, J.S. and A.G. Piersol, 1971. *Random Data: Analysis and Measurement Procedures*, John Wiley & Sons, pp. 407.

Borgman, L.E., 1972. Confidence intervals for ocean wave spectra. *Proc. 13th Int. Conf. Coast. Engng.*, **1**, 237-250.

Donelan, M. and W.J. Pierson,   1983. The sampling variability of estimates of spectra of wind-generated gravity waves. *J. Geophys. Res.*, **88**, 4381-4392.

Korteweg, D.J. and G. de Vries, 1895. On the change of form of long waves advancing in a rectangular canal and on a new type of long stationary waves. *Phil. Mag.*, **5**, 422-443.

Nadaoka, K., Beji, S. and Nakagawa, Y. 1994. A fully dispersive nonlinear wave model and its numerical solutions. *Proc. 24th Int. Conf. Coast. Engng.*, **1**, 427-441.

Nakamura, S. and Katoh, K., 1992. Generation of infragravity waves in breaking process of wave groups. *Proc. 23 th Int. Conf. Coast. Engng.*, 990-1003.